

Richard Bintanja · Roderik S. W. van de Wal  
Johannes Oerlemans

## A new method to estimate ice age temperatures

Received: 5 January 2003 / Accepted: 10 September 2004 / Published online: 11 December 2004  
© Springer-Verlag 2004

**Abstract** On glacial time scales, the waxing and waning of the Eurasian and North American ice sheets depend largely on variations in atmospheric temperature. As global sea level is primarily determined by the volume of these ice sheets, there is a direct (yet complex) relation between global sea level and the northern hemispheric (NH) temperature. This relation is essentially represented by a model of the NH ice sheets. We use a thermomechanical ice-sheet–ice shelf–bedrock model in conjunction with an inverse method to deduce a time series of NH temperature (from 120 kyr BP until present) that is consistent with the observed global sea level record. The advantage of this method is that it provides the annual mean surface air temperature averaged over the NH continents north of 40°N. The results reveal that ice age temperatures were 4–10°C lower than today, which agrees with other temperature reconstructions. However, reconstructed temperatures are comparatively low during the early stages of the glacial, a feature that is consistent with the rapid growth of the ice sheets. The sensitivity of the results for uncertainties in precipitation rate, in observed sea level and in some other model parameters is examined to quantify the error in reconstructed temperature. During the glacial period (120–15 kyr BP), surface air temperatures in the NH (north of 40°N) were  $7.2 \pm 1.5^\circ\text{C}$  lower than today's (interglacial) temperatures.

### 1 Introduction

During the last ice age, temperatures were much lower than today. At the Last Glacial Maximum (LGM) about 20 kyr ago, for instance, annual mean temperatures in Europe and North America were up to 20°C lower than the temperatures during the present interglacial (the Holocene), temperature differences being maximum in winter (Peyron et al. 1998). For a good understanding of (the causes of) climate variations, however, time series of climatic parameters are indispensable. At present, there are relatively few records of paleotemperature that cover the entire glacial period, and these are mostly records that have mainly regional significance (e.g. ice cores or lake sediment cores). Of course, such records have proven very valuable to investigate paleotemperature fluctuations, but for the investigation of global or hemispheric climate variations it would be beneficial if mean climatic values were available.

As an example of a local record, deep ice cores taken in Greenland and Antarctica (Jouzel et al. 1993; Johnsen et al. 1995) have yielded long records (> 100 kyr) of oxygen isotope variations, which have been translated into temperature signals using empirical relationships based on today's climatic conditions. As such, these records contain a wealth of high-resolution climatic information. The basic limitation with this procedure is that poorly understood mechanisms (for instance, changes in the seasonality of precipitation (e.g. Krinner et al. 2000)) may reduce the accuracy of the inferred temperature record. Hence, the interpretation of such a record is often not straightforward because it is a composite signal in which the various contributions may have changed over time (Cuffey et al. 1995).

Another source of oxygen isotope records involves the skeletal remains of benthic and planktonic foraminifera found in sediment cores taken in the deep ocean. These cores have provided us with very long records (up to a few million years), and have as such the potential to

---

R. Bintanja (✉) · R. S. W. van de Wal · J. Oerlemans  
Institute for Marine and Atmospheric Research Utrecht, Utrecht  
University, PO Box 80005, 3508 TA Utrecht, The Netherlands  
E-mail: R.Bintanja@phys.uu.nl  
Tel.: +31-30-2533259  
Fax: +31-30-2543163

yield climatic information over several glaciations. A general problem with these records is that it has been proven difficult to disentangle the effects of temperature and the depletion of ocean water to continental ice (which tend to occur synchronously) on the  $\delta^{18}\text{O}$ -ratio (Shackleton 2000).

A completely different method to construct a long temperature time series for the glacial period involves pollen assemblages (e.g. Guiot 1990) of fossil regional vegetation obtained from soil cores. As each plant species reacts in a specific manner to changes in regional temperature and precipitation, an inverse method is required to extract these meteorological variables from the community of floral species as represented by their pollen. A potential difficulty relates to the existence of modern analogs for plant species that are now extinct. Also, the range of climatic conditions that occurred over the period of the record may not be represented in today's vegetation mix.

These long temperature records have provided very useful insight into climate changes on ice age time scales. However, they suffer from two common limitations. First, the resulting temperature records mainly contain local or regional climatic information since the deposited material is affected mainly by the meteorological, climatological, geographical and other conditions at and in the vicinity of the coring location. Another point is that some of these temperature records are difficult to interpret, since the precise nature of the inferred temperature is unknown. Also the uncertainty is rarely estimated.

Obviously, the availability of a better-defined mean temperature record would be of great value for paleoclimatic research. In this paper we present a new and independent method that yields a time series of such a quantity (i.e. annual mean surface air temperature) over the last ice age (including a temporally varying uncertainty). The temperature that will be reconstructed is the annual mean temperature averaged over the NH land masses north of  $40^\circ\text{N}$  (henceforth loosely referred to as average NH temperature), and is as such a useful addition to the collection of paleotemperature data. To accomplish this, we use a coupled thermomechanical ice-sheet–ice shelf–bedrock model to simulate the (complex) relation between air temperature, ice volume and global sea level, and evaluate the temperature record from observed sea level data.

Until now, ice sheet models have been used in the following manner: the model is applied in, say, Eurasia and North America and is forced with a set of fixed atmospheric conditions (for e.g. the Last Glacial Maximum, LGM). Some models are set to run towards a steady-state, for which the simulated characteristics can then be compared to geomorphological data (e.g. Huybrechts and T'siobbel 1997). A more realistic approach is to perform transient experiments: either the ice sheet model is forced with one of the aforementioned temperature records over a longer period (e.g. one glacial cycle) (Bintanja et al. 2002), or it is coupled to a

simple atmospheric model (e.g. Tarasov and Peltier 1997). The result is a simulated sea level curve that can be compared with observed global sea level. Both approaches have invoked interesting discussions as to where (and also where not) the glacial ice sheets were situated (see e.g. Tarasov and Peltier 1997). In a more elaborate approach, Tarasov and Peltier (2004) use uplift and other geomorphological data to constrain the evolution of the thickness and extent of the Laurentide ice sheet during the deglaciation phase. It still remains a challenge to simulate NH ice sheets of the thickness and extent specified by geomorphological, geological and other data over an entire ice age cycle.

In this study, we use the ice-sheet–ice shelf–bedrock model the other way around. We take observed global sea level variations over the last 120 kyr as input, and derive a NH temperature record from that. This can be done because global sea level is influenced primarily by the waxing and waning of continental ice sheets in the NH. Geomorphological (Clarke et al. 1993) and glaciological (Tarasov and Peltier 1997; Huybrechts and T'siobbel 1997; Bintanja et al. 2002) studies suggest that the major contributors to the observed global sea level lowering during the last glacial were the Fennoscandian ice sheet in Northern Eurasia and the Laurentide–Corderillan ice sheet complex in North America. We apply the model to these regions and require that total simulated ice volume follows observed sea level. The model must adjust the mean surface air temperature to accomplish this. We may refer to this procedure as observationally constrained forward modelling, with the air temperature forcing at each model time step being guided by the sea level record. The result is a time series of temperature (anomaly) that is implicitly consistent with the observed sea level record. Again, the underlying assumption is that ice volume variations are governed by temperature variations, and that the most important variations in precipitation can be incorporated by relating them to temperature changes. Also changes in the dynamical flow regime and basal sliding conditions are considered of secondary importance for ice volume variations.

---

## 2 Methods and data

### 2.1 The coupled ice sheet–ice shelf–bedrock model

Fluctuations in ice sheet volume on glacial time scales are caused primarily by changes in temperature and precipitation and, to a lesser extent, by ice sheet dynamics (Tarasov and Peltier 1997). Temperature affects ice volume in a number of ways. Lower surface air temperatures inhibit surface melt, and increase the fraction of precipitation falling as snow, both of which favor ice sheet growth. In addition, lower ice temperatures reduce ice deformation (ice becomes stiffer) and basal sliding rates (ice gets frozen to the bed), enabling ice sheets to become thicker. Essentially, the coupled

ice sheet–ice shelf–bedrock model that we use represents the (complex) relation between temperature and ice volume.

A detailed description of the ice sheet–ice shelf–bedrock model is given by Bintanja et al. (2002), so here a summary of its most important characteristics will suffice. A 3-D ice sheet model is used to simulate growth and decay of continental ice, or grounded ice. It solves the prognostic equations for ice thickness (based on the shallow-ice approximation) and temperature, whereas the velocity field is evaluated diagnostically from internal deformation and basal sliding (e.g. Van de Wal 1999). Basal sliding is set to occur whenever the basal temperature is within 1°C of the pressure melting point, or when the ice sheet borders the open ocean, and depends on ice thickness and surface elevation gradients (Paterson 1994).

The albedo-mass balance feedback and the elevation-mass balance feedback are incorporated in the model (Bintanja et al. 2002), as described below. The surface mass balance is evaluated monthly. Ablation is taken to depend on surface air temperature, radiation (by forcing with spatially and seasonally varying solar radiation fluxes induced by orbital variations) and, notably, on surface albedo ( $\alpha$ ):

$$\alpha = \max(\alpha_{\text{gr}}, \alpha_{\text{sn}} - (\alpha_{\text{sn}} - \alpha_{\text{su}}) \exp[-\beta d]) \quad (1)$$

where  $\alpha_{\text{gr}}$ ,  $\alpha_{\text{sn}}$  and  $\alpha_{\text{su}}$  represent soil (0.2), snow (0.8) and surface (soil, glacier ice (0.45)) albedo, respectively,  $d$  is snow depth (in  $m$  water equivalent), and  $\beta$  is an empirical factor representing the effects of snow thickness and patchiness on albedo. Snow depth is an internal model variable that follows from the monthly cumulative mass balance, and is converted into ice by dividing with the ice density ( $917 \text{ kg m}^{-3}$ ).

Ice shelves are incorporated in a simple empirical manner, following Oerlemans and van der Veen (1984). In this method, ice shelf thickness is specified in terms of distance to the grounding line and ice thickness at the grounding line; dynamical aspects are neglected. Additionally, ice shelves are assumed to break up if temperatures become higher than  $-5^\circ\text{C}$ . This method favors the occurrence of ice shelves in narrow embayments, which is realistic. It is quite important to include ice shelves, even in a manner as simple as that used here, for two reasons. First, the possibility of grounding/ungrounding of ice shelves is an important feature of an ice sheet–ice shelf system. For instance, ice shelves enable ice sheets to expand across shallow seas and over continental shelves in a realistic fashion. Second, the surface elevation profile near ice sheet edges is more realistic (less steep) than in the case without ice shelves.

Vertical adjustments of the bed due to variable ice loads are incorporated through the elastic-lithosphere-relaxing-asthenosphere method (Le Meur and Huybrechts 1996). We employ global uniform values of the flexural rigidity of the lithosphere and of the relaxation time scale of the asthenosphere.

Simulations were restricted to Eurasia and North America (excluding Greenland), north of  $40^\circ\text{N}$ . Bintanja et al. (2002) simulated the global distribution of ice during the glacial period, and found that these regions consistently contributed about 85% to the total glacial–interglacial sea level difference (the changes are in phase), although we acknowledge that the contribution of the Antarctic ice sheet is still under debate (Tarasov and Peltier 1997; Huybrechts 2002). We simply added the remaining 15% to the total calculated ice volume to obtain the global ice volume, and thereby saved a significant amount of computing time by not having to simulate variations in ice volume globally. We believe that the error introduced by this assumption is small compared to the uncertainties in the paleo sea level data (to be discussed in the section Sea level data) and to other uncertainties associated with the method. The model uses realistic present-day topography; the initial state is assumed to be in local isostatic equilibrium. The model equations are solved on a rectangular  $20 \times 20 \text{ km}^2$  grid, with 4-year time steps. All model integrations started at 120 kyr BP, the end of the Eemian interglacial, with ice-free conditions throughout the model domain (which is in line with the geomorphological data).

## 2.2 Atmospheric forcing

The surface mass balance notably depends on temperature and precipitation, which have varied strongly over the last ice age. Temperature and precipitation changes are superimposed on the present-day monthly surface air temperature (i.e. the temperature at 2 m above the surface,  $T_s$ ) and precipitation fields (NCEP reanalysis data (Kalnay et al. 1996)). The NCEP-fields were bilinearly interpolated onto our  $20 \times 20 \text{ km}^2$  model grid (Bintanja et al. 2002), and we applied a correction for height differences using a lapse rate of  $-6.5 \text{ K km}^{-1}$ .

In this first attempt to extract temperatures from global sea level using an inverse method, we chose to incorporate climatic changes in the simplest possible manner to avoid complications with the interpretation of the reconstructed temperature record. With regard to temperature variations, we apply the same anomaly throughout the entire model grid, independent of season. In contrast, Bintanja et al. (2002) used a GCM-derived parameterization to account for latitudinally and seasonally varying changes in temperature, but these are deliberately ignored here. This means that spatial patterns of temperature do not change during our model ice age (apart from temperature changes induced by variations in surface height). We acknowledge that this is an important assumption, since summer temperature is the most important agent determining the ablation and thereby the extent of the ice sheet (e.g. the southern margin of the Laurentide Ice Sheet). Hence, for the standard runs the climate was changed in this simple manner to keep the results as transparent as possible. Uncertainties associated with this approach will be

investigated in the sensitivity analysis, by using the rudimentary climate model of Bintanja et al. (2002). For the sensitivity tests, we also applied a correction for changes in temperature seasonality (Bintanja et al. 2002):

$$\begin{aligned}\Delta T_{\text{mo}} &= \Delta T_{\text{ann}} \cdot f_s \\ &= \Delta T_{\text{ann}} \cdot \left\{ 1 + \gamma \left( \frac{\Delta T_{\text{mo}}(\text{GCM})}{\Delta T_{\text{ann}}(\text{GCM})} - 1 \right) \right\}\end{aligned}\quad (2)$$

where  $\Delta T_{\text{mo}}$  is the monthly temperature deviation,  $\Delta T_{\text{ann}}$  the annual temperature deviation as obtained from the inverse procedure. We have determined their ratio (as an average for the NH) using GCM output for the LGM and present-day, which was found to vary between 0.34 in summer and 1.61 in winter (Bintanja et al. 2002). This means that the seasonal cycle in temperature had a much larger amplitude during the LGM, and that the average cold conditions during the LGM can mainly be attributed to cold winters, which is confirmed by observations (Peyron et al. 1998). We can incorporate such changes in seasonality by using non-zero values of  $\gamma$ , as will be done in the sensitivity analyses. As stated before, changes in seasonality were ignored ( $\gamma=0, f_s=1$ ) in the standard runs. Note that the choice of  $\gamma$  affects the change in summer temperature, which governs the ablation and thereby the surface mass balance. Here it should be emphasized that model parameters can not be chosen randomly. For some unfavorable parameter settings the model is unable to produce the ice accretion required during strong growth stages, simply because precipitation rates are too low. With regard to sea level changes this is an asymmetric process: the model can always increase atmospheric temperatures further to melt more ice away, but higher accumulation rates cannot indefinitely be obtained by reducing temperature.

The surface temperature feeds into the ablation calculation and also serves as a boundary condition for the evaluation of the temperature distribution inside ice sheets. Ignoring atmospheric dynamics, changes in precipitation are related mainly to the moisture holding capacity of the troposphere, and hence to tropospheric temperature. We therefore need to estimate the free atmospheric temperature ( $T_a$ , just above the boundary layer). For this purpose, we use the relation of Jouzel and Melivat (1984), which reads (temperatures in K):  $T_s = 1.5 (T_a - 88.9)$ . This relation was originally derived for conditions with strong inversions, such as those prevailing over the Antarctic ice sheet. Similar (but not equal) near-surface conditions have most likely prevailed over the NH ice sheets (and over adjacent snow-covered regions) during the ice ages, and therefore this seems to be a feasible approach. However, it must be noted that, unlike Antarctica, the NH ice sheets were subject to a predominant westerly large-scale flow and baroclinic disturbances, which may have resulted in weaker inversions overall. The fact that this relation gives erroneous values over non-snow-covered regions is

unimportant since there the mass balance is negative anyway.

Precipitation changes are assumed to depend on deviations from present-day free atmospheric temperature ( $\Delta T_a$ , in K) according to:  $P = P_0 \cdot \zeta \Delta T_a$  where  $P$  is precipitation,  $P_0$  is the present-day precipitation rate and  $\zeta$  ( $=1.04$ ) is a factor that determines the rate of change (Huybrechts and T'siobbel 1997).  $\Delta T_a$  is composed of a hemispheric mean component and a local component, the latter being dependent only on the (evolving) surface elevation, which implies that, similar to temperature, spatial patterns in precipitation remain largely the same. Qualitatively, this relation has a sound empirical basis from ice-cores (Paterson 1994) and pollen analyses (Guiot 1990), theoretical considerations (Clausius-Clapeyron relation) and modelling studies (Rind 1986). It captures the most important effect on overall precipitation rates, i.e. a reduction in colder climates (the elevation-mass balance feedback). We realize, though, that there certainly have been periods during which some regions experienced increases in precipitation in spite of conditions being cooler, for instance because of (ice-sheet induced) changes in atmospheric circulation patterns (e.g. the southern margin of the Laurentide Ice Sheet) (Manabe and Broccoli 1985). Notice that storm-track precipitation is also sensitive to the meridional temperature gradient, which, in turn, is influenced by the insolation gradient.

### 2.3 Inverse method

It was chosen to reconstruct annual temperature over land even though summer temperature (more precisely, the average temperature during the period in which ablation occurs) governs the response of the ice masses (through the surface mass balance), simply because it is more relevant in a climatic sense and because its definition is unambiguous. It should also be noted that the method puts no constraints on air temperature fluctuations over the ocean (which presumably are less pronounced).

We use a quantitative inverse method that linearly relates a perturbation (relative to today's temperature) in average NH atmospheric temperature ( $\Delta T$ ) to the difference between modelled ( $H_{\text{sim}}$ ) and observed ( $H_{\text{obs}}$ ) global sea level:

$$\Delta T = \overline{\Delta T}_n + a(H_{\text{sim}} - H_{\text{obs}}) \quad (3)$$

where  $\overline{\Delta T}_n$  is the mean temperature perturbation over the previous  $n$  periods of 100 yr. In all experiments, the modelled ice volume (in sea level equivalents) is continuously compared with the observed sea level change 100 yr later, and the temperature is consequently adjusted so that the modelled ice volume changes in the desired direction. For instance, if the simulated sea level is too low, temperatures will be reduced so that

additional ice will form and sea level will drop. The model is essentially free to produce land ice anywhere it wants, provided that the observed sea level curve is followed. Each model experiment thus resulted in a 120 kyr temperature record that is fully consistent with the imposed sea level record. In Eq. (3), values of  $n$  ( $=20$ ) and of  $a$  ( $=2$ ) were optimized to suppress spurious high-frequency fluctuations in the resulting temperature record and to ensure that the system does not respond too slowly (for instance for low  $a$ -values). This essentially implies that the inverse method should have a time scale comparable to the response time scale of the physical system. As will be shown later, the differences between simulated and observed sea level are generally small (usually within 1 m).

As a test of how well this procedure works, we have made a temperature reconstruction using the SPEC-MAP sea level data. This reconstructed temperature record was then used to drive the model in normal mode (i.e. the model is forced by temperature and calculates ice volume and sea level changes). It was found that the sea level curve thus obtained matched very well the one that was used as input (differences  $< 0.5$  m). It can therefore be concluded that the method is self-consistent.

## 2.4 Sea level data

The first detailed temporal record of late Pleistocene sea level variations was presented by Imbrie et al. (1984). This record was based on oxygen isotope ratio fluctuations in benthic foraminifera in marine sediment cores. However, this  $\delta^{18}\text{O}$ -signal not only depends on global ice volume but also on local seawater temperature. Shackleton (2000) used the same type of data and attempted to correct for temperature by subtracting the temperature signal from the Vostok (Antarctica) record, which he identified with high-latitude surface ocean temperature.

The  $\delta^{18}\text{O}$ -ratio method has the advantage that a high-resolution record of relative sea level is obtained. However, well-dated sea level markers are required to obtain absolute sea level. Such markers are indeed available for the last ice age, but only for a limited number of points in time (Lambeck et al. 2002). Generally, absolute sea level can be obtained from raised shorelines or fossil reefs, but only if they are unaffected by isostatic adjustment processes following fluctuations in land ice cover. Results should be corrected for possible tectonic movements.

As shown by Lambeck and Chappell (2001), there are abundant absolute sea level data during the deglaciation stage of the last glacial (from approximately 18 kyr BP to present), during which global sea level has risen about 100 m. Prior to that, reliable data are scarce. Lambeck and Chappell (2001) present absolute sea level data obtained from Huon Peninsula, New Guinea, and Bonaparte Gulf, Australia. In the period 120–15 kyr, there

are currently only about 20 well-dated absolute global sea level data.

Figure 1a shows the smoothed (frequencies smaller than 5 kyr have been filtered out) and interpolated sea level curves that were obtained with the methods discussed above. There seems to be overall agreement between the three curves, although at some instances differences amount to as much as 50 m! This illustrates that global sea level during the last ice age is still not accurately known. A noticeable difference between the SPECMAP sea level curve and more recent estimates occurs for the period 60–20 kyr (Linsley 1996), during which SPECMAP sea levels appear to be too low. On the other hand, the three curves agree on three main points: (1) there was a rapid fall in sea level of 40–60 m following the end of the Eemian interglacial (the onset of the last glaciation), (2) sea level appeared to fluctuate on 5–10 kyr timescales, and these variations are superimposed on a more or less gradual decrease in sea level prior to the LGM, and (3) sea level has risen about 120 m following the LGM.

All three sea level curves depicted in Fig. 1a will be used to reconstruct the temperature record; however, only the SPECMAP curve will be used to study the sensitivity of the method.

---

## 3 Temperature reconstructions

### 3.1 Results for the various sea level estimates

The reconstructed temperature (anomalies) resulting from the three sea level curves are depicted in Fig. 1b. Reconstructed temperatures during the glacial were 2–12°C lower than today. As we will show later, this range is in broad agreement with other estimates. Another striking feature is the marked variability in reconstructed temperature. The temperature fluctuations are obviously induced by simultaneous variations in sea level, relatively cold periods being associated with local minima in sea level. In fact, strong cooling stages generally precede local minima in sea level and are associated with the expansion of the ice sheets. This is because temporal changes in ice volume are proportional to the mass balance (and hence the rate of change in ice volume), which depends strongly on temperature (in particular through ablation). A prerequisite for this is the highly variable climate during the glacial period, as a result of which the ice sheet mass balance is governed by fluctuations in surface mass balance; dynamics are only of secondary importance.

Fluctuations in ice volume and sea level lag those in temperature. In other words, ice sheets require a temperature reduction in order to expand; once sufficiently large, ice sheets create their own cold climate (even if the effect of increased albedo values on air temperature is disregarded, as is done here) which enable them to persist without further cooling. Another interesting

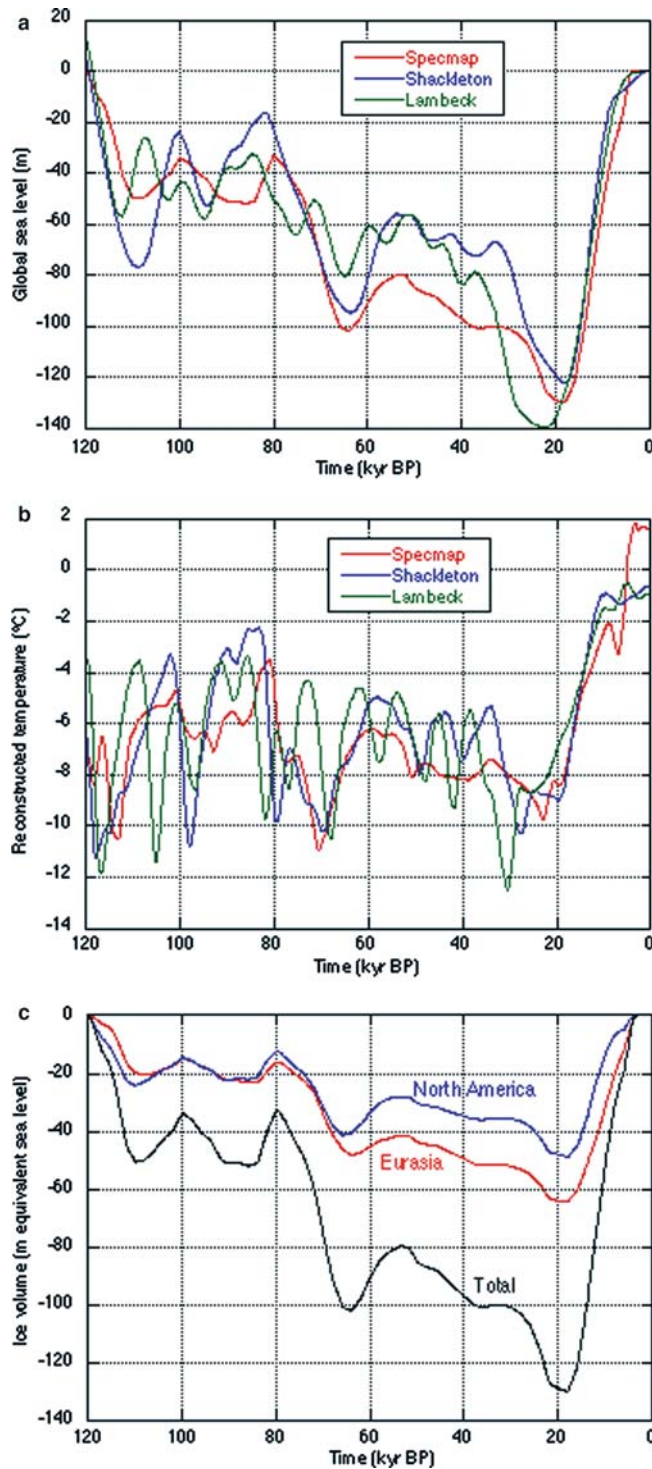


**Fig. 1** a Variation in global sea level over the last 120 kyr. Past sea level stands have been reconstructed using benthic  $\delta^{18}\text{O}$  data (Imbrie et al. 1984) (SPECMAP; in red) in combination with atmospheric  $\delta^{18}\text{O}$  from ice cores (Shackleton 2000; in blue), and a combination of raised-reef sequences and other local rebound-corrected sea level data (Lambeck and Chappell 2001; in green). Each curve was plotted on its original time scale. b Reconstructed temperatures for the three sea level records. c Modelled ice volumes in North America and Eurasia for the SPECMAP reconstruction, as well as the total (global) ice volume, for which 15% was added to the sum of NAM and EAS ice volume

feature is that simulated temperatures are determined primarily by the rate of change of sea level, and only to a smaller degree by the actual sea level. As a result, the sea level record with the strongest variations (“Lambeck”) yields the most vigorous fluctuations in reconstructed temperature. This is related to the smoothing of the sea level records.

A potential complication is that some of the variations in global sea level that were deduced from the  $\delta^{18}\text{O}$ -records may not be directly related to temperature at all. In particular short-term fluctuations may instead be caused by mechanisms that are not included in the model, such as ice sheet instabilities, abrupt surges and ice discharges related to Heinrich ice-rafting events (MacAyeal 1993). This is the main reason why we filtered out short-term variations (period  $< 5$  kyr) in sea level. Using such rapidly changing sea levels would have resulted in unrealistically strong fluctuations in the concurrent temperature record. A further advantage of smoothing is that random errors related to the “measurement” of the sea level data are eliminated. Despite all this, we acknowledge that there remains a degree of subjectiveness in the smoothing procedure, even though we made sure that the 5 kyr limit is roughly equal to the response time scale of the physical model.

The simulated ice volumes for the SPECMAP case are shown in Fig. 1c. The simulated total ice volumes in the two regions, North-America (NAM) and Eurasia (EAS), and their combined volume (15% added to yield a global value) is depicted in terms of equivalent sea level. During the first part of the glacial period, NAM contains most ice, whereas in the latter stages the situation is reversed. During later stages of the glacial period, the ice volume in EAS becomes much larger than in NAM. At least for the LGM this is not a very realistic situation, as it was estimated that the ice volume stored in NAM was about 2.5 times larger than in EAS (Tarasov and Peltier 1997). This ratio was probably much smaller in the early stages of the last ice age (during which the Fennoscandian Ice sheet may have reached its greatest extent (Svendsen et al. 1999)), but it nevertheless indicates that in the present configuration our model overestimates the amount of ice in EAS and, since the total ice volume is dictated by the sea level curve, it underestimates the NAM ice volume. This is a result that is not uncommon among ice sheet models (e.g. Huybrechts and T’siobbel 1997) and ice sheet reconstructions. It can probably be attributed to problems with the atmospheric forcing. We should note here that we treat NAM and EAS in exactly the same manner; it would be quite easy to vary a few model parameters and tune each region to the correct ice volume. This, however, would not lead to more insight as to why the standard model produces incorrect ice volumes. At the same time it must be noted that we disregard local climate responses that may be typical for one region but not for the other, such as the drying of eastern sections of Siberia resulting from the built-up of the

Fennoscandian Ice Sheet, and spatial differences in ocean heat flux due to variations in the thermohaline circulation of the ocean. In the next section we will discuss the consequences of this deficiency for the temperature reconstruction.

### 3.2 Sensitivity tests

#### 3.2.1 Precipitation rates

One of the most important uncertainties with the present method is that changes in ice volume are assumed to be caused by temperature fluctuations only (including temperature-related effects on precipitation). In reality, precipitation changes caused by other factors may have contributed as well. For instance, precipitation patterns may have been modified by natural climate variations, by changes in availability of open water moisture sources and by changes in the atmospheric circulation due to the presence of large ice sheets that deflected the westerly jet. For instance, it is known that the southern marginal zone of the Laurentide ice sheet probably received more moisture than it does today (Manabe and Broccoli 1985). Another example of this is the cold and very dry climate prevailing in the Kara Sea and Taymyr Peninsula region during the LGM, which was invoked by the obstruction of the westerly atmospheric flow by the Fennoscandian–Barents Sea ice sheets to the west (Siegert et al. 1999). This relates to the fact that large ice sheets in the midlatitudes presumably received more moisture on the westerly slopes than on the easterly slopes, thereby invoking a westward transgression of the ice sheets (Sanberg and Oerlemans 1983). Such mechanisms are disregarded in the present study; we only take into account temperature-governed deviations from the present-day precipitation fields, as mentioned above. Ideally, one should use a (simple) climate model to generate precipitation (and temperature) fields (e.g. Tarasov and Peltier 1997; Huybrechts and T'siobbel 1997) that would fit into the framework of the present methodology, but our aim is to explore the simple approach used here.

Therefore, we will restrict ourselves to quantify the effects of changes in precipitation on the reconstructed temperature. First, we will focus on the sensitivity of the reconstructed temperature to inaccuracies in the initial precipitation fields. For this purpose, we have repeated the calculations for the SPECMAP sea level curve for doubled and halved precipitation rates (Fig. 2). Clearly, increased precipitation rates lead to higher ice age temperatures (i.e. reduced cooling). This is because the surface mass balance is then positive for higher temperatures, which enables ice sheets to grow and persist in relatively mild conditions. In other words, if for some reason ice sheet growth was accompanied by increased precipitation rates, the temperatures required to reproduce the observed sea level lowering were substantially higher than in the case of constant precipitation. In

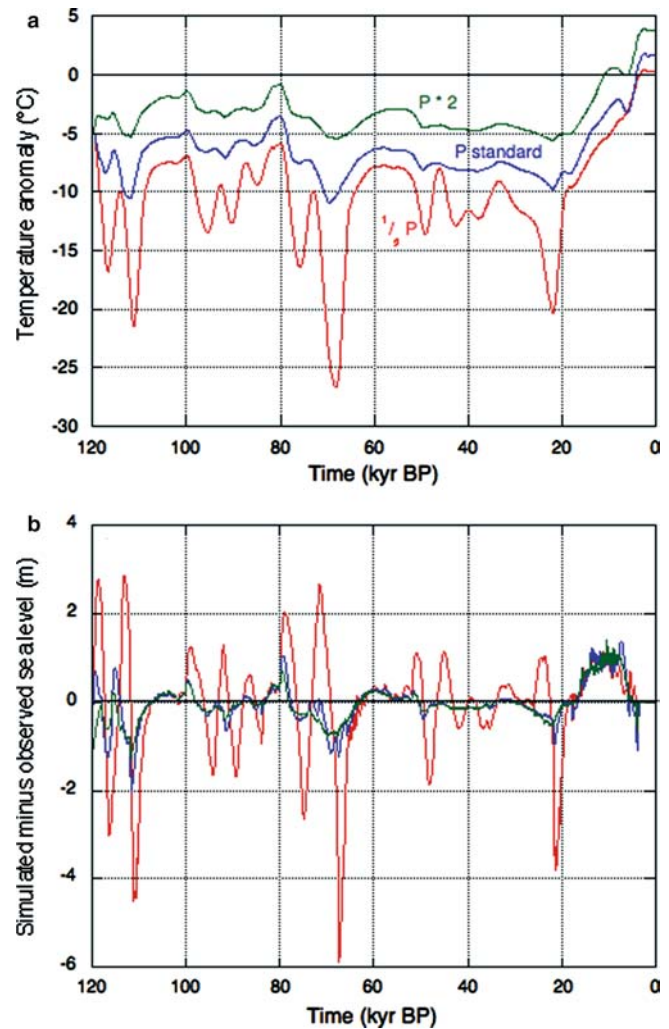


**Fig. 2** **a** Reconstructed temperature anomalies for the standard case (blue), the doubled precipitation case (green) and the case in which precipitation was reduced by 50% (red), and **b** the difference between simulated and observed global sea level for the three cases. All three cases use the SPECMAP sea level curve

contrast, in relatively dry environments comparatively large temperature reductions are required to enable ice sheet expansion. Incidentally, this indirectly illustrates the difficulty in forming ice sheets in cold and very dry environments. In the case of reduced precipitation rates reconstructed temperatures become as low as  $-25^{\circ}\text{C}$ , and also the variability in temperature is increased significantly (Fig. 2).

Figure 2b shows the difference between simulated and observed sea level. For the standard and increased precipitation scenarios, this difference remains smaller than 2 m at all times, and simulated sea level is always slightly ahead of observed sea level. In contrast, the difference is up to 6 m in the reduced precipitation scenario, illustrating the difficulty of the model to ‘follow’ the observed sea level curve in this case. Hence, dry environments also increase the response time of the ice sheet–mass balance system. Although the changes

applied here are unrealistically large, these tests illustrate how changes in precipitation can alter the reconstructed temperatures.

Another illustrative test is to change the value of  $\zeta$  (standard value: 1.04) in the formulation that relates changes in precipitation to temperature changes (which specifies that the moisture content of air reduces in cold environments). We have changed the value of  $\zeta$  to 1.00 (no change in precipitation rate) and to 1.06 (larger values resulted in a climate that was too dry to build up ice sheets at the rate dictated by the sea level curves), again for the SPECMAP case. Figure 3a shows the resulting temperature reconstructions. In case of  $\zeta = 1.00$ , reconstructed temperatures are not as low as in the standard case. This is because precipitation rates remain high in spite of the low temperatures, which enable ice sheets to become and remain large in relatively mild conditions. Alternatively, lower temperatures result when precipitation rates are reduced more strongly in cold conditions ( $\zeta = 1.06$ ).

Lower than standard temperatures (by  $0.7^\circ\text{C}$  on average, not shown) are also found if, as a sensitivity experiment, free atmospheric temperature is set equal to surface air temperature, thereby ignoring the relation of Jouzel and Melivat (1984). This results in lower temperatures at which the precipitation is evaluated, and, as a result, relatively dry conditions that inhibit growth of the ice sheets, and additional cooling to obtain the required ice volume.

### 3.2.2 Reconstruction of precipitation changes

We have shown that precipitation changes may have a strong influence on the reconstructed temperatures. What if sea level variations were entirely due to changes in precipitation (at today's temperatures)? This, however, is not a realistic situation, because the air is then simply too warm for the precipitation to fall as snow. Probably the next best scenario is to prescribe an existing temperature record (e.g. the one derived from  $\delta^{18}\text{O}$  record of the Vostok ice core) and let the model find the precipitation changes ( $\Delta P$ ) that are consistent with the observed sea level curve (Fig. 3b). These precipitation changes (again, mean values for the NH continents north of  $40^\circ\text{N}$ ) should be interpreted as the changes required when the Vostok temperature anomaly is representative for the entire NH. Hence, if values of  $\Delta P$  are larger than 1, the prescribed temperature was too high to generate the required amount of ice, which the model then compensates for by increasing the precipitation rate. This is precisely what happens between 120 and 110 kyr BP, when almost a doubling in precipitation is apparently needed to produce land ice at the rate consistent with the observed sea level lowering. During the remainder of the glacial period values of  $\Delta P$  remain between 0.4 and 1.1. If these values are compared with the precipitation history from Les Eschets, France (Fig. 3b) as obtained from pollen analyses (Guiot 1990),

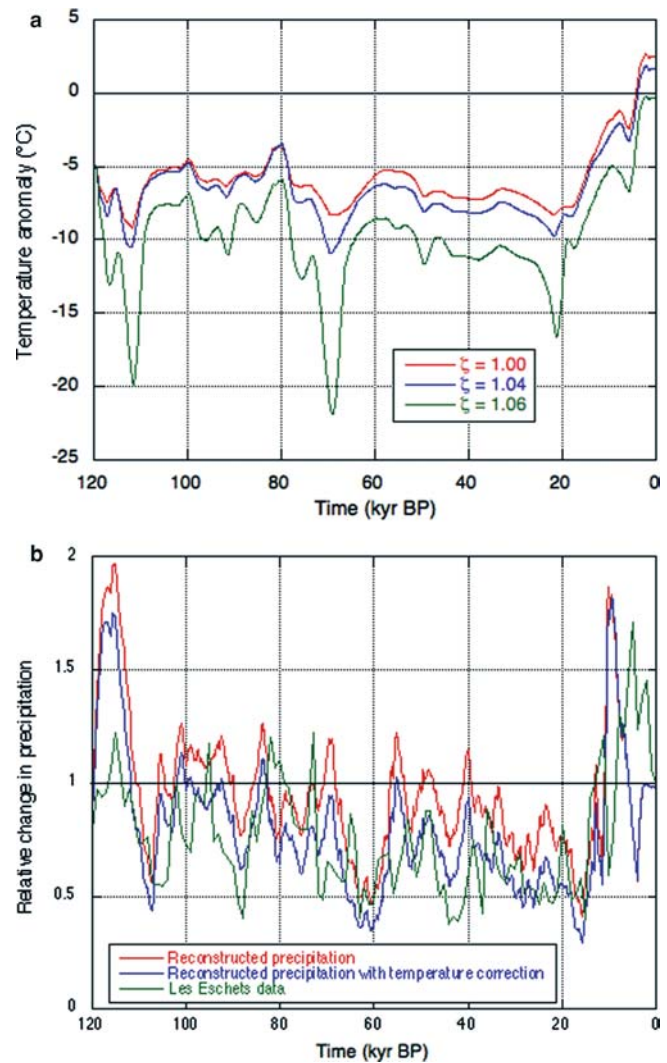


**Fig. 3** **a** Reconstructed temperature anomalies for the standard case (blue), and two cases in which the model parameter  $\zeta$  was changed (red, green). Higher  $\zeta$ -values mean that precipitation rates will be strongly reduced in cold climates. All three cases use the SPECMAP sea level curve. **b** Reconstructed precipitation rates (the relative change relative to present-day) for the SPECMAP sea level curve. The Vostok temperatures (Jouzel et al. 1993) are prescribed. The red line indicates how precipitation must have varied in order to follow the SPECMAP sea level curve, while the blue line shows the actual precipitation rates (including temperature effects). Observed precipitation for Les Eschets, France, as obtained from pollen analysis (Guiot 1990), is shown in green

we can conclude that the range of precipitation change is fairly realistic, except for the first 10 kyr when precipitation rates in France were approximately the same as today. This does not rule out, however, the possibility that precipitation rates near the ice sheet nucleation centres could have been relatively high, but a large-scale increase in precipitation rate during this early stage does not seem likely. It can also not be ruled out that precipitation changes had an influence on ice volume and sea level during the coldest stages of the ice age (about 110–20 kyr ago).

In general, reconstructed temperatures may be affected by changes in precipitation. Ideally, one would retrieve temperature and precipitation simultaneously from the sea level record. However, it is unclear how this should be achieved within the framework of this method (i.e. how can the contributions of changes in temperature and precipitation be objectively distinguished?). The problem is clearly underconstrained. Therefore, we will stick to the concept of reconstruction of temperature only, and accept that errors due to the neglect of precipitation changes remain. In the section Error Estimation, we will attempt to estimate the error in reconstructed temperature, part of which will be due to effects of precipitation.

### 3.2.3 The seasonal temperature cycle and other changes in climate

A further uncertainty is introduced by changes in the amplitude of the seasonal cycle of temperature that may have occurred during the ice age. As stated above, climate modelling studies as well as proxy temperature data show that ice age temperatures were especially cold in winter, and that reductions in summer temperatures may have been relatively moderate. We incorporate such effects by using nonzero values of  $\gamma$  (see Eq. (2)). The results of two sensitivity experiments are shown in Fig. 4a. The effects of incorporating only moderate changes in seasonality are quite large, with reconstructed temperatures being much lower than in the standard case ( $\gamma=0$ ). The effect of milder summer temperatures is that the model needs stronger annual temperature reductions to keep ablation rates low and to produce the required amount of ice. In case of  $\gamma=1$  (not shown), this effect results in extremely low reconstructed temperatures. This may be attributed to the fact that, in reality, changes in seasonality will not be uniform. Instead, they should vary spatially, especially over the different parts of an ice sheet. A future study will address this important issue.

To test whether the model is sensitive to climate feedbacks, we have used the highly parameterized climate ‘model’ of Bintanja et al. (2002), which is based on GCM experiments for the LGM and the present. This model has two components: (1) a term that enhances the temperature response over ice sheets (in addition to the height-effect) to mimic the strong temperature gradients over ice-land boundaries, especially in summer, and (2) a term that makes the climate response latitude-dependent (stronger temperature changes in polar regions). Figure 4b shows the results for both experiments. If the ice sheets are allowed to become substantially colder than their surroundings, reconstructed mean temperatures are generally higher than in the standard case. This is because ice ablation rates are reduced, enabling the mass balance to be more positive so that less cooling is required to attain the prescribed ice volume. Obviously, this is counteracted as lower temperatures reduce pre-

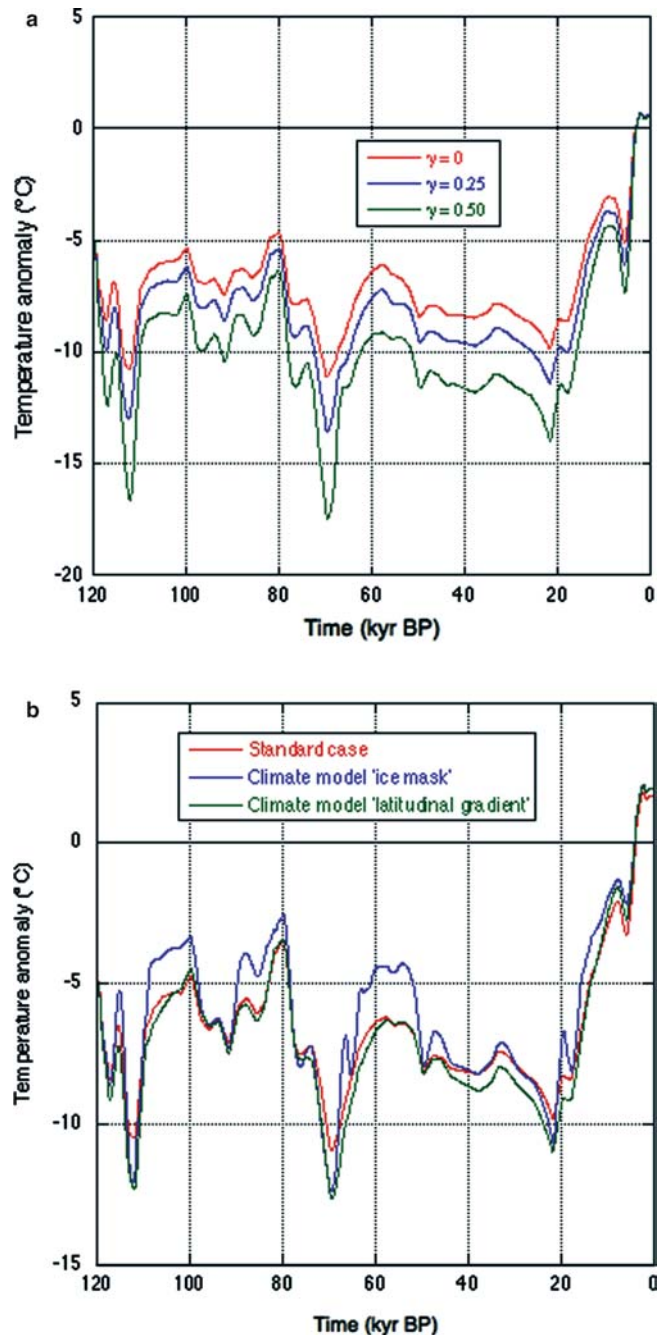


**Fig. 4** **a** Reconstructed temperature anomalies for the standard case (red), and two cases in which the model parameter  $\gamma$  was changed (blue, green). Nonzero  $\gamma$ -values mean that the amplitude of the seasonal cycle is increased in cold climates. **b** Reconstructed temperature anomalies for the standard case (blue), and two cases in which the climate model parameterization of Bintanja et al. (2002) are applied: ‘ice mask’, in which temperatures over the ice sheets are reduced, and ‘latitudinal gradient’, in which the temperature change varies latitudinally (strongest changes near the poles). All cases use the SPECMAP sea level curve

cipitation rates, but only during brief times of strong expansion and cooling this is strong enough to offset the ablation-effect. The latitude-effect causes a slight reduction in the reconstructed temperature, a result of

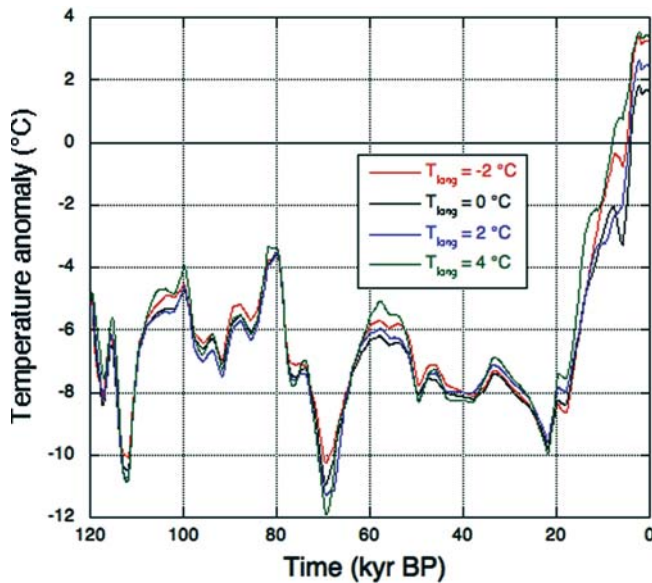


**Fig. 5** Reconstructed temperature anomalies for four values of  $T_{\text{long}}$ . The standard case is for  $T_{\text{long}}=0^{\circ}\text{C}$ . All cases use the SPECMAP sea level curve

the warming of the southern parts of the ice sheets (relative to the standard case), which enhances ablation rates in these regions. This is partly offset by cooler temperatures in the north. In both cases, the average effect is relatively small.

### 3.2.4 Spatial distribution of the ice sheets

Another difficulty relates to the simulated distribution of the various ice masses. As stated before, the simulated ice volume in EAS is somewhat greater than that in NAM at the LGM, whereas geomorphological (Clarke et al. 1993) and rebound studies (Peltier 1994) suggest that the ice volume in NAM should have been much larger (perhaps about 2.5 times as large) than in EAS. How does this discrepancy affect the results? To test this, we introduce a new parameter ( $T_{\text{long}}$ ) that specifies a longitudinal gradient in air temperature ( $T_{\text{long}}$  has no physical basis). If  $T_{\text{long}}$  equals  $2^{\circ}\text{C}$ , then the atmosphere over the NAM-domain is  $2^{\circ}\text{C}$  colder than over the EAS-domain (the computational domains occupy the same surface area), while the average temperature remains the same as in the standard case. Hence, NAM is then one degree colder than the mean, and EAS one degree warmer. We performed three additional experiments, with values of  $T_{\text{long}}$  of  $-2$ ,  $2$  and  $4^{\circ}\text{C}$  (in the standard experiment  $T_{\text{long}}=0^{\circ}\text{C}$ ), using the SPECMAP sea level data.

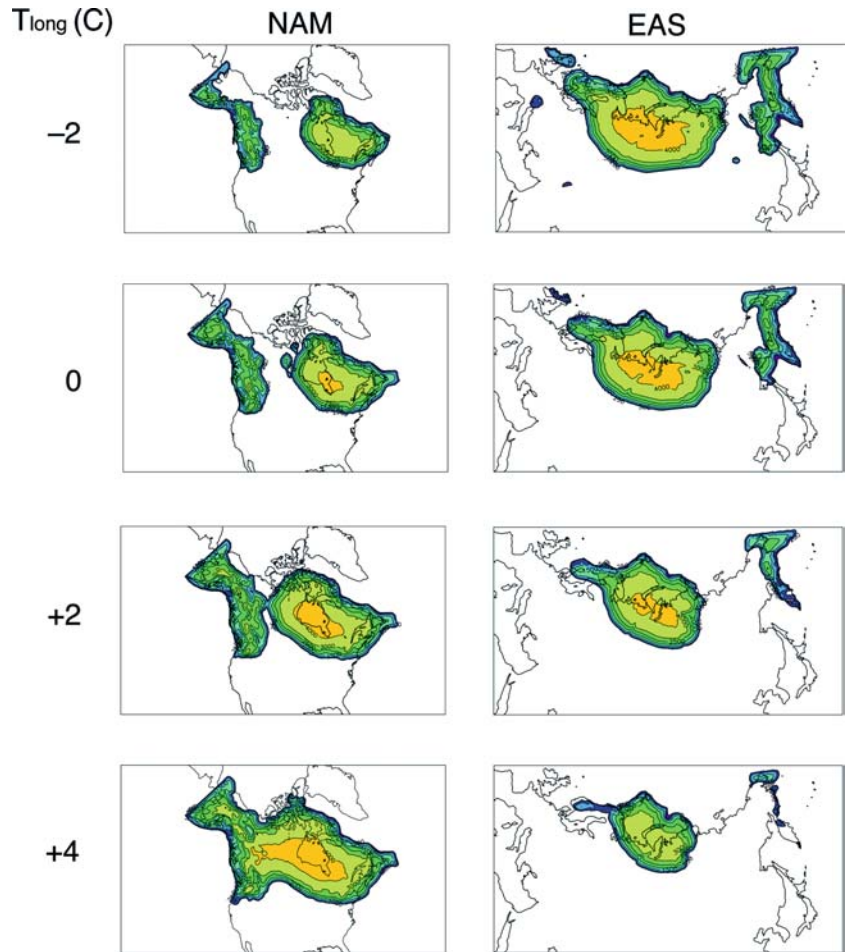
Figure 5 shows the time series of reconstructed temperatures for these experiments. Clearly, the effect of imposing longitudinal temperature gradients is relatively small, with differences between the four experiments only rarely exceeding  $1^{\circ}\text{C}$ . In contrast, the effects on the simulated ice distributions are enormous. Figure 6

shows the spatial distribution of the simulated ice sheets at LGM. In North America, ice is centred in the mountainous western side of the continent (the Cordilleran Ice Sheet, CIS) and in the eastern side (the Laurentide Ice Sheet, LIS). In Eurasia, there were the Fennoscandian Ice Sheet (FIS), which extended well into the northern parts of western Russia and the continental shelf of the Arctic Ocean (Barents Sea), and a smaller ice sheet complex over the mountainous Kamchatka peninsula. As expected, the ice volume in NAM increases with increasing  $T_{\text{long}}$  (and decreasing local temperatures), whereas ice cover in EAS shrinks. With increasing  $T_{\text{long}}$ , the CIS and LIS end up as one huge ice sheet covering much of the northernmost part of NAM. This is probably the configuration that resembles best the LGM boundaries from geomorphological evidence (Clarke et al. 1993), even though the centre of the ice sheet is probably too thick to account for the observed postglacial rebound data in the Hudson Bay region (Peltier 1994, 1996). Similarly, the thickness and extent of the FIS reduce considerably with increasing  $T_{\text{long}}$ . There is probably too little ice in Northern Europe (Kleman and Hättestrand 1999), because the FIS extends too far to the east (Svendsen et al. 1999) in all cases.

However, the central point here is that for the purpose of reconstructing ice age temperatures it does not matter much where the ice sheets were located. Figures 5 and 6 clearly demonstrate that the ice sheets can be moved around while the reconstructed temperature hardly changes. In other words, the reconstructed temperature is hardly influenced by uncertainties in the location of the ice sheets, at least in our model. This may at least partly be due to the neglect of local climate effects, such as changes in continentality, oceanic influences and changes in atmospheric flow patterns. This result implies that we need not bother too much about where the simulated ice sheets are located. In this particular sense the method appears to be quite robust. Future studies should show if this conclusion will hold in more complex model settings.

In Fig. 7 the total volumes of the continental ice in NAM and EAS at LGM are depicted, as well as the surface area occupied by both as a function of  $T_{\text{long}}$ . The LGM ratio of ice volume in NAM and EAS (equal to 2.5 according to Tarasov and Peltier 1997) is attained at a value of  $T_{\text{long}}$  of about  $3.25^{\circ}\text{C}$  (the vertical hatched line in Fig. 7). In that case, the volume of the NAM ice sheets is about  $4 \times 10^{16} \text{ m}^3$ , which is significantly larger than the  $(2.4\text{--}3.0) \times 10^{16} \text{ m}^3$  range in ice volume estimated by Tarasov and Peltier (1997, 2004) but closer to the simulated ice volume  $(34.2 \pm 2.3 \cdot 10^{15} \text{ m}^3)$  of Marshall et al. (2002). Since our NAM ice volume is probably an overestimate at the required ratio, there is no self-consistent solution that complies with current knowledge of LGM ice volumes. In this respect, it is worthwhile to note that at any point in time some portions of the ice sheet will be below sea level, which means that its actual impact on sea level is smaller than if all ice was above sea

**Fig. 6** Simulated ice thickness distributions ( $m$ ) at the LGM in North America (NAM) and Eurasia (EAS) for four values of  $T_{\text{long}}$ . The standard case is for  $T_{\text{long}} = 0^\circ\text{C}$ . All cases use the SPECMAP sea level curve



level. This effect is considered in translating total volume of the ice sheets (which includes this submerged ice) into equivalent sea level.

### 3.3 Error estimation

In the previous section, it was shown that possible errors in the location of the ice sheets hardly affect the temperature reconstruction. We have identified two main contributions to the error in reconstructed temperature. The first relates to the uncertainty in the actual value of the past sea level. Notably, the three estimates used here vary widely (Fig. 1a), even though the overall form of the curves is similar. Additionally, each individual sea level curve is subject to errors in magnitude and dating. Lambeck and Chappell (2000) estimate the errors in their sea level reconstruction at 10–20%. We will assume that the accuracy in absolute sea level of each curve is 20%, even though the differences between the three curves suggest that that errors may be larger than that for some periods. We nevertheless applied changes of 20% to the three sea level curves in the SPECMAP case (Fig. 8), and recalculated the temperature. Figure 8 shows that this leads to changes in temperature that are generally smaller than

$1^\circ\text{C}$  (these deviations are referred to as  $\sigma_{\text{hsl}}$ ). The average uncertainty associated with a 20% change in global sea level is only  $0.4^\circ\text{C}$ .

The second and most important source of error is associated with uncertainties in the ice sheet model and the forcing. We performed a comprehensive sensitivity test to determine for which model/forcing variables, varied within their range of uncertainty (based on empirical data, theoretical considerations and model tests), the model was most sensitive. The four most important parameters were selected, two of which are internal model variables (basal sliding parameter and the parameter  $\beta$  that relates snow depth to surface albedo), while the other two are associated with the forcing (parameter  $\zeta$ , which relates precipitation to temperature changes, and parameter  $\gamma$  that determines the seasonality of the temperature forcing). The latter is important because climate model studies and paleoclimatic reconstructions (e.g. Kageyama et al. 2001) have demonstrated that climate-change induced temperature changes are largest in winter. Based on empirical data, theoretical considerations and model tests (conditions should not become too dry to accommodate the rapid build-up of ice in some periods) we established a range of uncertainty for each of these four parameters. We ran the model for 52 combinations of minimum, mean and

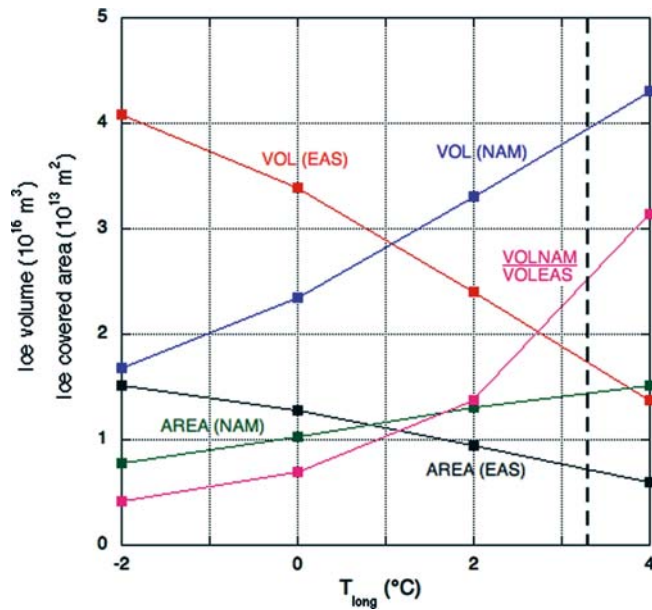


Fig. 7 Ice volume and the area occupied by ice at the LGM in North America (NAM) and Eurasia (EAS) as a function of  $T_{\text{long}}$ . Also shown is the ratio of the volume in NAM and in EAS, and the vertical dashed line indicates where this ratio equals 2.5

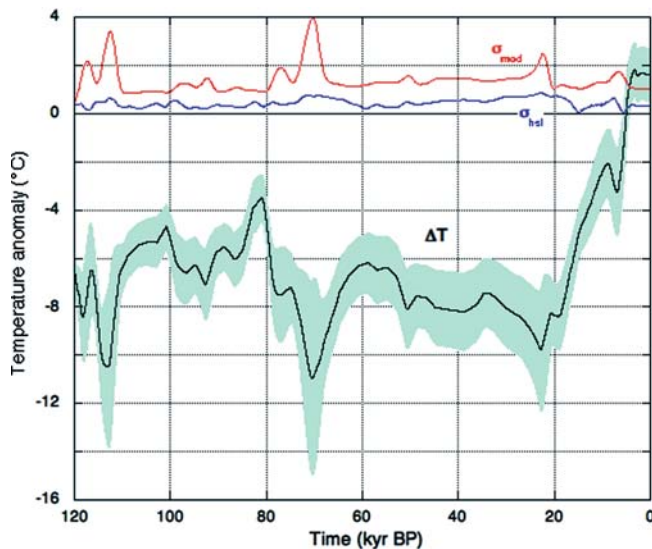


Fig. 8 Standard deviations for a 20% uncertainty in sea level (blue) and for model/forcing uncertainties (red), while the black curve depicts the reconstructed temperature anomaly with the envelope denoting the associated combined standard deviation, for the SPECMAP reconstruction

maximum values of the four parameters for the SPEC-MAP case (see Table 1).

The resulting 52 temperature records were then averaged, which provided the standard deviation ( $\sigma_{\text{mod}}$ ) induced by modelling uncertainties (see Fig. 8). Clearly, errors induced by modelling uncertainties are larger than those invoked by uncertainties in the observed sea level. Also, errors peak when the temperature change is

maximum, which demonstrates that ice sheets are particularly sensitive under rapidly changing conditions. We have determined  $\sigma_{\text{mod}}$  for each of the three sea level curves, and combined them with  $\sigma_{\text{hsl}}$  to obtain the total standard deviation. Figure 8 shows the reconstructed temperature for the SPECMAP sea level data and the associated total error. The average total error is 1.5°C. The temperature reconstructions for each of the three sea level estimates and the associated variances were averaged to yield the best estimate of the average NH temperature and its uncertainty.

### 3.4 Comparison with other paleotemperature estimates

In Fig. 9 the best estimate of the present study is shown and compared with three other paleotemperature records. The first two were deduced from  $\delta^{18}\text{O}$  or deuterium records in deep ice cores in central Greenland (GRIP; Johnson et al. 1995; Cuffey et al. 1995) and central Antarctica (Vostok; Jouzel et al. 1993). With regard to GRIP temperatures it is noted that recent studies (Dahl-Jensen et al. 1998) have shown that surface temperatures at the Greenland ice sheet summit during the LGM were much lower than those originally deduced from  $\delta^{18}\text{O}$  data. The third record is obtained from pollen assemblages in a lake core in Les Eschets, France (Guiot 1990). As stated in the introduction, these records are in principle representative only for the region in which they were taken, which means that an (unknown) part of the difference will be due to the fact that Fig. 9 compares regional with hemispheric mean temperatures.

Nevertheless, some interesting inferences can be made. The most important result is that the range of temperature deviation during the ice age (4–10°C below present) compares well with the other estimates, save the revised GRIP temperatures which are representative strictly for the summit region of the Greenland ice sheet. From GCM studies of the LGM climate it is known that the summit regions of the various ice sheets were significantly colder than the mean (with respect to present-day). A comprehensive review of LGM temperature in Eurasia from models and data was made by Kageyama et al. (2001). They show that, on average, NH midlatitude to polar LGM temperatures were roughly 10°C lower than today, with strong seasonal and spatial variations. This indicates that our LGM temperature of  $-8.3 \pm 1.6^\circ\text{C}$  below present is not too unrealistic. Remember also that we have filtered out high-frequency variations, so the fact that short-time scale fluctuations in the other records fall outside this range is to be expected. The present method is simply inadequate to study rapid climatic changes.

Another noticeable aspect of the comparison relates to the comparatively low temperatures in the beginning of the last ice age as found in our study. How can this discrepancy be explained? The drop in reconstructed temperature would be less pronounced if part of the ice

**Table 1** Minimum, mean and maximum values of the four selected parameters used to estimate the error of the method associated with model uncertainties. The sliding parameter is a factor by which sliding velocities are multiplied

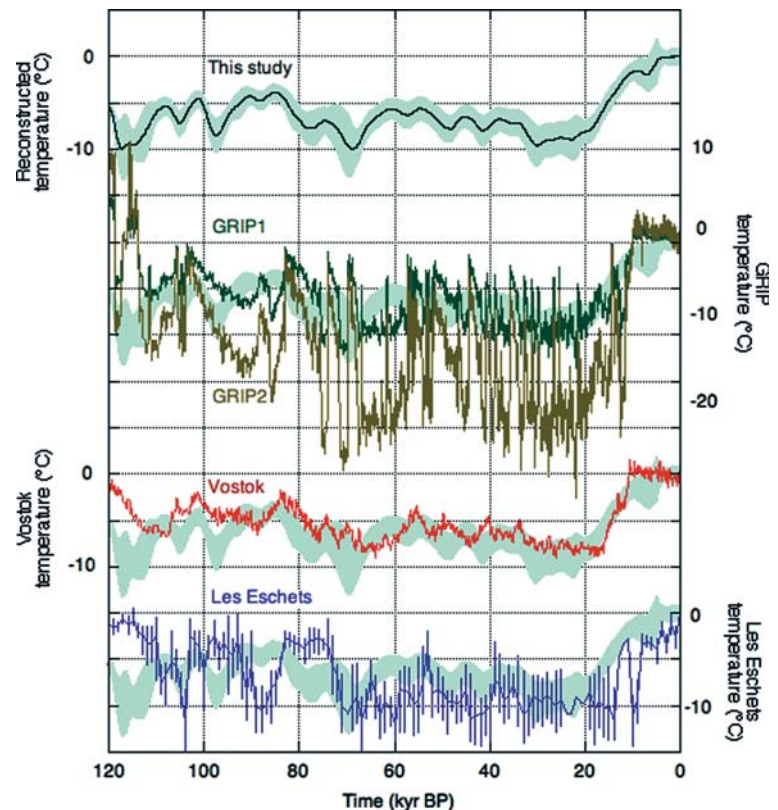
Parameter	Minimum	Mean	Maximum
Sliding	1	10	100
$\beta$ (Relates albedo to snowdepth)	5	15	30
$\gamma$ (Determines seasonality of temperature)	0	0.25	0.50
$\zeta$ (Relates precipitation to temperature changes)	1.0	1.04	1.06

sheet build-up could be attributed to increased precipitation, as shown in Fig. 3b. Some modelling studies indeed suggest that the precipitation at 120 kyr BP might have been higher than today, because of increased baroclinic wave activity (Dong and Valdez 1995) and poleward moisture transport, possibly in conjunction with ocean feedbacks (Khodri et al. 2001). Assuming that Vostok temperatures can be applied to the NH, we showed that precipitation rates need to be doubled to match the observed increase in ice sheet volume (Fig. 3b). Even higher increases in precipitation are required when initially milder temperatures (such as those of GRIP and Les Eschets) are used. In all these cases, the simulated and observed global sea level agree less favorably than in the original reconstruction. Existing paleo-precipitation records, such as the Les Eschets record, albeit far away from inception regions, do not

exhibit the required increases in precipitation. All this indicates that increases in precipitation may have only played a minor role in the growth of early glacial ice sheets, and that the simulated rapid temperature drop at the beginning of the glacial is realistic. We therefore believe that the discrepancy between our result and the other records may for a large part be attributed to uncertainties in the interpretation of the local temperature reconstructions. For instance, the GRIP record suffers from stratigraphic disturbances for ice older than 110 kyr BP. Also the pollen record from Les Eschets has its difficulties, as the chronology of the record before 30 kyr is linked to the isotope chronology of marine cores and is therefore not independently established. This would only leave the Vostok record, which however cannot be taken as representative for the NH during inception.

If real, what does the exceptional drop in temperature that accompanied the 50–80 m fall in sea level between 120 and 110 kyr BP (equivalent to 50–80 cm per century) imply? North Atlantic ocean sediment cores indicate that high-latitude sea surface temperatures (SST) were already lowered by as much as 4°C before inception of the ice sheets occurred (Cortijo et al. 1994, 1999); this cooling is probably associated with a southward migration of deep water formation regions. Forsström and Punkari (1997) found evidence of large-scale glaciation in Scandinavia during the early stages of the last glacial, and note that a 6–7°C cooling is required to achieve this. General circulation model (GCM) studies of the early

**Fig. 9** Reconstructed average NH temperature (*black*) for the three sea level curves combined, with the envelope denoting the total standard deviation. Other temperature reconstructions have been included for comparison: original  $\delta^{18}\text{O}$ -derived temperature for the GRIP site, Greenland (Johnsen et al. 1995) in *green* (GRIP1); revised  $\delta^{18}\text{O}$ -derived temperature for the GRIP site using borehole thermometry (Cuffey et al. 1995), in *brown* (GRIP2)  $\delta^{18}\text{O}$ -derived temperature for Vostok, Antarctica (Jouzel et al. 1993) in *red*; temperature derived from pollen assemblage in lake sediments in France (Guiot 1990) in *blue*



glacial climate indicate that reduced SST may have induced a cooling of 4–6.5°C in the mid-latitude to polar continental regions of the NH (Dong and Valdez 1995), the magnitude of which is sufficient for ice sheet inception to occur (Dong and Valdez 1995; Khodri et al. 2001; Yoshimori et al. 2002). Hence, observed low SST and reduced surface air temperatures in the subpolar regions of the NH, as inferred from GCMs, indicate that conditions were favorable for the system to begin forming ice sheets. However, GCMs cannot be used to predict how the climate developed after the initial formation of the NH ice sheets. Our results suggest that a continual and intensifying cooling is required to build up ice sheets at the rate suggested by the global sea level records. This incessant cooling may have been caused by strengthening of the albedo-temperature feedback once there was land ice that survived the summer season. Changes in ocean circulation (reduction in thermohaline overturning) (Khodri et al. 2001) and in vegetation (southward expansion of tundra) (Yoshimori et al. 2002) may also have contributed to the prolonged cooling.

The timing of events depends strongly on the accuracy (including the dating) of the sea level curves. This becomes clear when the period around 80 kyr BP is inspected. All local records exhibit a local maximum in temperature at or just before 80 kyr, whereas in our reconstruction the corresponding maximum occurs at least 5 kyr earlier. The agreement is much better when only the SPECMAP case is considered (Fig. 8), so the mismatch may at least partially be attributed to the choice of sea level curves that are used to perform the reconstructions.

For the second half of the glacial period, including the LGM, the overall agreement appears to be favorable. Also the increasing temperature during deglaciation seems to be captured well.

#### 4 Concluding remarks

A new and independent method is presented to estimate ice age temperatures. The basic concept of this method is that mean NH temperature (of the land masses north of 40°N) is constrained by variations in global sea level. This is because NH temperature changes largely drive the ice sheets in North America and Eurasia, which, in turn, govern global sea level fluctuations. A numerical ice sheet–ice shelf–bedrock model is used in conjunction with a formal inverse method to convert the observed time series of global sea level (from 120 kyr BP to present) into a concurrent temperature record. We have used a comparatively simple atmospheric forcing: temperature anomalies were assumed to be independent on location and season, and also the spatial distributions of temperature and precipitation were kept similar to present-day patterns.

Sensitivity tests demonstrate that the assumption of a temporal invariant precipitation rate (temperature-induced variations were included, but those invoked by

changes in atmospheric dynamics were not) may affect the reconstructed temperature: if for some reason precipitation rates were higher than today, the climate required for the ice sheets to reach the volume prescribed by global sea level would be less cold. The tests also reveal that possible errors in the locations of the model ice sheets hardly affect the resulting temperature record. The reconstructed temperature does hardly change if an increase in ice sheet volume in North America and a decrease in Eurasia (to comply better with geomorphologically inferred distributions) is enforced.

Two main sources of error were identified: uncertainties in the sea level data and uncertainties in the parameters of the model (parameters related to basal sliding, albedo–snowdepth coupling, temperature seasonality and temperature-precipitation coupling). We quantified the effect of both uncertainties on the resulting temperature time series. According to our best estimate, the average NH annual surface air temperature (over the continents north of 40°N) over the period 120–15 kyr (roughly the last ice age) is  $-7.2 \pm 1.5^\circ\text{C}$  below present.

We compared our temperatures with other temperature time series over the same period (those obtained from  $\delta^{18}\text{O}$  ratio in ice cores and from pollen analyses in soil sediments). Even though these records are representative only for the regional climate, the agreement with our NH mean temperature appears to be fairly good. The most striking deviation occurs in the beginning of the glacial period (120–110 kyr BP), for which our method produces comparatively low temperatures. These cold conditions are consistent with the exceptional strong decrease in sea level (and hence with the build-up of continental ice), although we cannot rule out the possibility that local increases in precipitation have contributed to the early ice sheet growth. In the light of the many simplifications that were made (in particular those associated with the atmospheric forcing) it will be worthwhile to infer how the results of this study compare to a similar inverse approach with a more realistic ice–climate coupling.

**Acknowledgements** We are grateful to S. Johnsen, J. Jouzel, and J. Guiot for providing the data used in Figs. 4 and 9. Financial support was provided by the Netherlands Organisation of Scientific Research (NWO), in the framework of the PULS funding programme of the Earth and Life Sciences department (ALW). Insightful comments were provided by S. Marshall, L. Tarasov and an anonymous reviewer.

#### References

- Bintanja R, van de Wal RSW, Oerlemans J (2002) Global ice volume variations through the last glacial cycle simulated by a 3-D ice-dynamical model. *Q Int* 95–96: 11–23
- Clarke PU, et al (1993) Initiation and development of the Laurentide and Cordilleran ice sheets following the last interglacial. *Q Sci Rev* 12:79–114
- Cortijo E, et al (1994) Eemian cooling in the Norwegian Sea and North-Atlantic Ocean preceding continental ice-sheet growth. *Nature* 372: 446–449

- Cortijo E, Lehman S, Keigwin L, Chapman M, Paillard D, Labeyrie L (1999) Changes in meridional temperature and salinity gradients in the North Atlantic Ocean (30–72°N) during the last interglacial period. *Paleoceanography* 14:23–33
- Cuffey KM, Clow GD, Alley RB, Stuiver M, Waddington ED, Saltus RW (1995) Large Arctic temperature change at the Wisconsin-Holocene Glacial transition. *Science* 270:455–458
- Dahl-Jensen D, Mosegaard K, Gundestrup N, Clow GD, Johnsen SJ, Hansen AW, Balling N (1998) Past temperature directly from the Greenland Ice Sheet. *Science* 282:268–271
- Dong B, Valdez PJ (1995) Sensitivity studies of Northern Hemisphere glaciation using an atmospheric general circulation model. *J Clim* 8:2471–2496
- Forsström L, Punkari M (1997) Initiation of the last glaciation in Northern Europe. *Q Sci Rev* 16:1197–1215
- Guiot J (1990) Methodology of the last climatic cycle reconstruction in France from pollen data. *Paleogeogr Paleoclimatol Paleoecol* 80(1):49–69
- Huybrechts P (2002) Sea-level changes at the LGM from ice-dynamic reconstructions of the Greenland and Antarctic ice sheets during glacial cycles. *Q Sci Rev* 21:203–231
- Huybrechts P, T'siobbel S (1997) A three-dimensional climate–ice-sheet model applied to the Last Glacial Maximum. *Ann Glaciol* 25:333–339
- Imbrie J et al (1984) The orbital theory of Pleistocene climate: support from a revised chronology of the marine  $\delta^{18}\text{O}$  record. In: Berger AL (Ed) *Milankovitch and Climate*. Reidel, Dordrecht, pp 269–305
- Johnsen SJ, Dahl-Jensen D, Dansgaard W, Gundestrup NS (1995) Greenland temperatures derived from GRIP borehole temperature and ice core isotope profiles. *Tellus* 47B:624–629
- Jouzel J et al (1993) Extending the Vostok ice-core record of paleoclimate to the penultimate glacial period. *Nature* 364:407–412
- Jouzel J, Melivat L (1984) Deuterium and oxygen 18 in precipitation: modelling of the isotopic effects during snow formation. *J Geophys Res* 89:11749–11757
- Kageyama M et al (2001) The last glacial maximum climate over Europe and western Siberia: a PMIP comparison between models and data. *Clim Dyn* 17:23–43
- Kalnay E et al (1996) The NCEP/NCAR 40-year reanalysis project. *Bull Am Meteor Soc* 77(3):437–471
- Khodri M et al (2001) Simulating the amplification of orbital forcing by ocean feedbacks in the last glaciation. *Nature* 410:570–574
- Kleman J, Hättestrand C (1999) Frozen-bed Fennoscandian and Laurentide ice sheets during the Last Glacial Maximum. *Nature* 402:63–66
- Krinner G, Raynaud D, Doutriaux C, Dang H (2000) Simulations of the Last Glacial Maximum ice sheet surface climate: implications for the interpretation of ice core air content. *J Geophys Res* 105 (D2):2059–2070
- Lambeck K, Chappell J (2001) Sea level change through the last glacial cycle. *Science* 292:679–686
- Lambeck K, Esat TM, Potter EK (2002) Links between climate and sea levels for the past three million years. *Nature* 419:199–206
- Le Meur E, Huybrechts P (1996) A comparison of different ways of dealing with isostasy: examples from modelling the Antarctic ice sheet during the last glacial cycle. *Ann Glaciol* 23:309–317
- Linsley BK (1996) Oxygen-isotope record of sea level and climate variations in the Sulu Sea over the past 150,000 years. *Nature* 380:234–237
- MacAyeal DR (1993) Binge/purge oscillations of the Laurentide ice sheet as a cause of the North-Atlantic Heinrich events. *Paleoceanography* 8(6):775–784
- Manabe S, Broccoli AJ (1985) The influence of continental ice sheets on the climate of the ice age. *J Geophys Res* 90:2167–2190
- Marshall SJ, James TS, Clarke GKC (2002) North American ice sheet reconstructions at the Last Glacial Maximum. *Q Sci Rev* 21:175–192
- Oerlemans J, van der Veen C (1984) *Ice sheets and climate*. Reidel, Dordrecht, p 217
- Paterson WSB (1994) *The physics of glaciers*. Pergamon, Tarrytown, p 480
- Peltier WR (1994) Ice age paleotopography. *Science* 265:195–201
- Peltier WR (1996) Mantle viscosity and ice-age ice sheet topography. *Science* 273:1359–1364
- Peyron O, Guiot J, Cheddadi R, Tarasov P, reille M, de Baulieux JL, Bottema S, Andrieu V (1998) Climate reconstruction in Europe for 18,000 yr B.P. from pollen data. *Q Sci Res* 49:183–196
- Rind D (1986) The dynamics of warm and cold climates. *J Atmos Sci* 43:3–24
- Sanberg JAM, Oerlemans J (1983) Modelling of Pleistocene European ice sheets: the effect of upslope precipitation. *Geologie en Mijnbouw* 62:267–273
- Shackleton NJ (2000) The 100,000-year ice-age cycle identified and found to lag temperature, carbon dioxide, and orbital eccentricity. *Science* 289:1897–1902
- Siegert MJ, Dowdeswell JA, Melles M (1999) Late Weichselian glaciation of the Russian high Arctic. *Q Res* 52:273–285
- Tarasov L, Peltier WR (1997) Terminating the 100 kyr ice age cycle. *J Geophys Res* 102:21665–21693
- Tarasov L, Peltier WR (2004) A geophysically constrained large ensemble analysis of the deglacial history of the North American ice-sheet complex. *Q Sci Rev* (in press)
- Van de Wal RSW (1999) The importance of thermodynamics for modeling the volume of the Greenland ice sheet. *J Geophys Res* 104:3887–3898
- Yoshimori M, Reader MC, Weaver AJ, McFarlane NA (2002) On the causes of glacial inception at 116 ka BP. *Clim Dyn* 18:383–402